JOURNAL OF BACTERIOLOGY, Apr. 1995, p. 2057–2063 Vol. 177, No. 8
0021-9193/95/$04.00+0

Association of Molybdopterin Guanine Dinucleotide with *Escherichia coli* Dimethyl Sulfoxide Reductase: Effect of Tungstate and a *mob* Mutation

RICHARD A. ROTHERY,[1] JOANNE L. SIMALA GRANT,[1] JEAN L. JOHNSON,[2] K. V. RAJAGOPALAN,[2] AND JOEL H. WEINER[1]*

Medical Research Council Group in the Molecular Biology of Membranes, Department of Biochemistry, University of Alberta, Edmonton, Alberta, Canada T6G 2H7,[1] and Department of Biochemistry, Duke University, Durham, North Carolina 27710[2]

Received 7 December 1994/Accepted 13 February 1995

We have identified the organic component of the molybdenum cofactor in *Escherichia coli* dimethyl sulfoxide reductase (DmsABC) to be molybdopterin (MPT) guanine dinucleotide (MGD) and have studied the effects of tungstate and a *mob* mutation on cofactor (Mo-MGD) insertion. Tungstate severely inhibits anaerobic growth of *E. coli* on a glycerol-dimethyl sulfoxide minimal medium, and this inhibition is partially overcome by overexpression of DmsABC. Isolation and characterization of an oxidized derivative of MGD (form A) from DmsABC overexpressed in cells grown in the presence of molybdate or tungstate indicate that tungstate inhibits insertion of Mo-MGD. No electron paramagnetic resonance evidence for the assembly of tungsten into DmsABC was found between $E_h = -450$ mV and $E_h = +200$ mV. The *E. coli mob* locus is responsible for the addition of a guanine nucleotide to molybdo-MPT (Mo-MPT) to form Mo-MGD. DmsABC does not bind Mo-MPT or Mo-MGD in a *mob* mutant, indicating that nucleotide addition must precede cofactor insertion. No electron paramagnetic resonance evidence for the assembly of molybdenum into DmsABC in a *mob* mutant was found between $E_h = -450$ mV and $E_h = +200$ mV. These data support a model for Mo-MGD biosynthesis and assembly into DmsABC in which both metal chelation and nucleotide addition to MPT precede cofactor insertion.

Escherichia coli, when grown anaerobically on glycerol with dimethyl sulfoxide (DMSO) as a respiratory oxidant, develops a respiratory chain terminated by a menaquinol:DMSO oxidoreductase (DMSO reductase; DmsABC) (35). This enzyme is a heterotrimeric complex iron-sulfur molybdoenzyme comprising a molybdenum cofactor-containing catalytic subunit (DmsA; 87.4 kDa), an [Fe-S] cluster-containing electron-transfer subunit (DmsB; 23.1 kDa), and an integral membrane anchor subunit (DmsC; 30.8 kDa) (3). DmsABC is an excellent example of a recently identified group of bacterial complex iron-sulfur molybdoenzymes, which includes *E. coli* nitrate reductases A and Z (NarGHI and NarZYV) (6, 7), formate dehydrogenase N (FdnGHI) (2), and *Wolinella succinogenes* polysulfide reductase (PsrABC) (18). Sequence comparisons between DmsA and a large number of bacterial molybdoenzymes indicate that this subunit binds the molybdenum cofactor and is the site of DMSO reduction (3, 33, 35).

Significant advances in the elucidation of molybdenum cofactor biosynthesis and insertion into bacterial molybdoenzymes have recently been made (12, 22, 23, 27, 31). The final step of cofactor biosynthesis in *E. coli* appears to be the addition of a guanine nucleotide to molybdo-molybdopterin (Mo-MPT), resulting in the formation of Mo-MPT guanine dinucleotide (Mo-MGD), which is the form of the cofactor found in the mature *E. coli* molybdoenzymes (15, 23). The gene product responsible for this addition is encoded by the *mob* locus (15). DmsABC does not support anaerobic growth on DMSO in a *mob* mutant (4), suggesting that the cofactor present is Mo-MGD not Mo-MPT. It has been proposed that, at least in the case of NarGHI, nucleotide addition occurs after Mo-MPT insertion (27), suggesting that in a *mob* mutant, inactive molybdoenzymes may be present with bound Mo-MPT. It is not clear why this proposed form of NarGHI has no detectable nitrate reductase activity. It would be interesting to determine if DmsABC contains Mo-MPT in a *mob* mutant.

The molybdenum cofactor is also able to provide ligands to tungsten instead of molybdenum in a number of enzymes (16, 29, 30). In the hypothermophilic *Archaebacteria*, tungsten is the preferred metal in aldehyde:ferredoxin oxidoreductase and formaldehyde:ferredoxin oxidoreductase (16). In the methanogen *Methanobacterium wolfei*, the cofactor of formylmethanofuran dehydrogenase is able to ligate either tungsten or molybdenum, and in both cases, the enzyme retains activity (29, 30). The formate dehydrogenase of *Clostridium thermoaceticum* also assembles a tungsten-containing cofactor to form an active enzyme (11). In *E. coli*, growth in the presence of tungstate results in the synthesis of an empty cofactor (MPT) which accumulates in the cytoplasm (1). This MPT is able to reconstitute *Neurospora crassa* nitrate reductase activity in the *nit-1* assay in the presence of added molybdate, but it is unable to reconstitute *E. coli* nitrate reductase activity (28). It is not clear whether MPT or MGD (metal-free cofactor) is inserted into DmsABC or into *E. coli* molybdoenzymes in general.

In this paper, we describe the identification of the molybdenum cofactor in DmsABC as Mo-MGD. We have investigated the effect of a *mob* mutation and tungstate on the assembly of Mo-MGD into DmsABC. We show that the effect of a *mob* mutation on the assembly of cofactor into DmsABC appears to

* Corresponding author. Mailing address: MRC Group in the Molecular Biology of Membranes, Department of Biochemistry, 474 Medical Sciences Building, University of Alberta, Edmonton, Alberta, Canada T6G 2H7. Phone: (403) 492-2761. Fax: (403) 492-0886. Electronic mail address: joel.weiner@ualberta.ca.

TABLE 1. Bacterial strains and plasmids used in this study

Strain or plasmid	Genotype	Source or references
E. coli strains		
HB101	*supE44 hsdS20* (r_B^- m_B^-) *recA13 ara-14 proA2 lacY1 galK2 rpsL20 xyl-5 mtl-1*	Laboratory collection
RK5208	F^- *araD139 lacU169 gyrA thi rpsL mob207*::Mu *cts*	31, 32
Plasmids		
pBR322	Amp^r *lacZ′*	Pharmacia
pDMS159	pBR322 Amp^r $(dmsABC)^+$	5
pDMS160	pBR322 Amp^r $(dmsABC)^+$	25

be different from its reported effect on cofactor assembly into NarGHI (27).

MATERIALS AND METHODS

Bacterial strains and plasmids. The *E. coli* strains and plasmids used in this study are listed in Table 1. pDMS159 (5) and pDMS160 (25) both contain the entire *dmsABC* operon cloned into pBR322. pDMS160 lacks a noncoding 1.66-kbp fragment 3′ to *dmsC*.

Growth of cells. Cells were grown anaerobically either on a glycerol-DMSO (GD) minimal medium (4) or on a glycerol-fumarate (GF) minimal medium (10). For biochemical and biophysical analyses, *E. coli* HB101 was grown at 37°C for 48 h in 20-liter batch cultures on GF medium in the presence of either 5 μM ammonium molybdate or 15 mM sodium tungstate. *E. coli* RK5208 was grown at 23°C for 72 h on GF minimal medium. Cell growth at 37°C on GD minimal medium in the presence of tungstate was assessed with a Klett-Summerson spectrophotometer equipped with a no. 66 filter, and the cultures were supplemented either with 20 μM ammonium molybdate or up to 100 mM sodium tungstate.

Preparation of membrane vesicles. Cells were harvested and washed, and membranes were prepared by French pressure cell lysis and differential centrifugation (25) in 50 mM MOPS (morpholinepropanesulfonic acid)–70 mM trimethylamine-*N*-oxide (TMAO)–5 mM EDTA (pH 7.0). The buffer used during the French pressing step contained 0.2 mM phenylmethylsulfonyl fluoride. Prior to biochemical and biophysical characterizations, the buffer was exchanged for 100 mM MOPS–5 mM EDTA (pH 7.0).

Purification of DmsABC. DmsABC was purified from membranes by detergent extraction and ion-exchange chromatography on a DE-52 column as described previously (9). The nonfluorescent detergent $C_{12}E_8$ was used in place of Triton X-100.

Enzyme and protein assays. TMAO-dependent oxidation of reduced benzyl viologen ($BV \cdot^+$) was determined as previously described (9). Protein concentrations were determined by the method of Lowry et al. (19), modified by the inclusion of 1% (wt/vol) sodium dodecyl sulfate in the incubation mixture to solubilize membrane proteins (20).

Identification of MGD. Purified DmsABC was desalted on a Sephadex G-25 column, and MGD was identified by conversion to dicarboxamidomethyl-MPT (camMPT)-GMP and form A MPT-GMP (14, 15). Both products were degraded with nucleotide pyrophosphatase to yield GMP and the corresponding pterin, camMPT or form A MPT. Fluorescence and absorption spectra were compared with standard spectra of GMP, form A MPT, and camMPT.

Fluorescence assay for form A MPT. The presence of molybdenum cofactor in experimental samples was assayed by acid denaturation of membrane vesicles followed by I_2 and KI oxidation (15). For assays of membrane-associated molybdenum cofactor, 20 mg of total membrane protein was used as starting material. Prior to the recording of fluorescence spectra, small aliquots (100 to 200 μl) of the acid-denatured iodine-oxidized extracts were added to 3 ml of 1 M ammonium hydroxide. Fluorescence spectra were recorded with a Perkin-Elmer LS50 luminescence spectrometer. Excitation and emission wavelengths were as described in the individual figure legends.

EPR spectroscopy. Electron paramagnetic resonance (EPR) spectra were recorded with a Bruker Spectrospin ESP300 spectrometer equipped with an Oxford Instruments ESR-900 flowing helium cryostat. Samples were prepared in calibrated 3-mm-internal-diameter quartz tubes as described in the individual figure legends. Redox-poised samples were prepared as described by Cammack and Weiner (9), and the following mediators were used at a concentration of 50 μM: quinhydrone (midpoint E_h [$E_{m,7}$] = +286 mV), 2,6-dichlorophenolindophenol ($E_{m,7}$ = +217 mV), thionine ($E_{m,7}$ = +60 mV), phenazine ethosulfate ($E_{m,7}$ = +55 mV), duroquinone ($E_{m,7}$ = +7 mV), methylene blue ($E_{m,7}$ = −11 mV), resorufin ($E_{m,7}$ = −50 mV), indigodisulfonate ($E_{m,7}$ = −125 mV), anthraquinone-2-sulfonic acid ($E_{m,7}$ = −225 mV), phenosafranine ($E_{m,7}$ = −255 mV), BV ($E_{m,7}$ = −360 mV), and methyl viologen ($E_{m,7}$ = −440 mV). The redox potential was measured with a platinum measuring electrode with a calomel reference electrode, and the potential was adjusted with small additions of sodium dithionite and potassium ferricyanide solutions. After redox equilibration, samples were transferred to quartz EPR tubes and rapidly frozen in liquid nitrogen.

RESULTS

Identification of MGD in DmsABC. The *mob* locus is known to be responsible for the addition of GMP to Mo-MPT in *E. coli* (15). Earlier studies indicated that *mob* was required for DmsABC function, suggesting that Mo-MGD is the cofactor present in the enzyme (4). The cofactor in DmsABC was confirmed to be Mo-MGD by extraction and conversion to the stable derivatives camMPT-GMP and form A MPT-GMP. The UV absorption maxima of camMPT-GMP are at 250 and 277 nm (Fig. 1). The absorption maximum at 250 nm is characteristic of a guanine nucleotide attached to MPT (14). The form A MPT-GMP showed the expected 10-fold increase in fluorescence after treatment with nucleotide pyrophosphatase (15) (data not shown). The amount of MGD per mole of DmsA was quantitated by extracting equivalent amounts of form A MPT from DmsABC and the DMSO reductase of *Rhodobacter sphaeroides*. On a molar basis, purified DmsABC contains 0.26 mol of MGD per mol of enzyme. However, we have shown by mass spectroscopy and EPR that the molybdenum concentration of membranes containing overexpressed DmsABC is stoichiometric with the concentration of enzyme determined by EPR spin quantitations of the DmsB [4Fe-4S] clusters (see Discussion) (25a).

Effect of tungstate on respiratory growth on DMSO. Figure 2 shows the effect of tungstate on respiratory growth on GD minimal medium of *E. coli* HB101 cells transformed with pBR322 and pDMS160. HB101/pBR322 cells readily grow on a GD minimal medium in the presence of 20 μM molybdate.

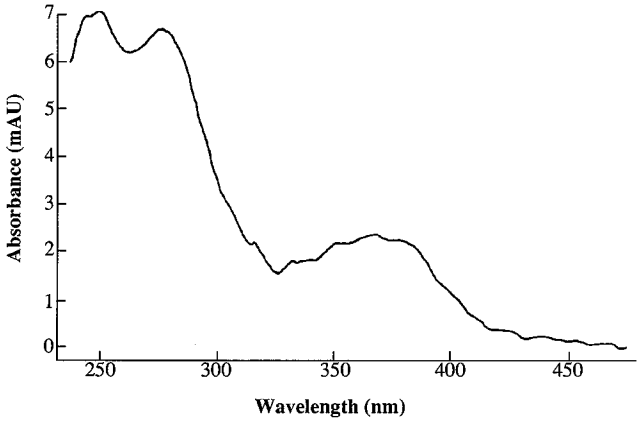

FIG. 1. Absorption spectrum of oxidized camMPT-GMP prepared from purified DmsABC in 50 mM ammonium acetate (pH 6.8). mAU, milli-absorbance units.

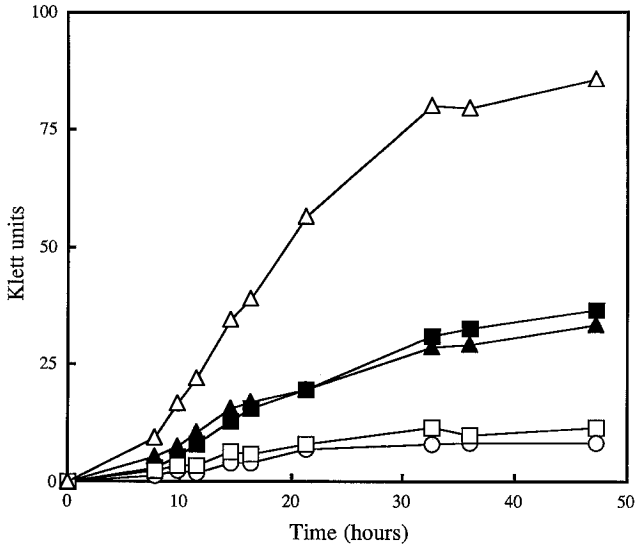

FIG. 2. Effect of tungstate on anaerobic growth on GD minimal medium. △, HB101/pBR322 grown on molybdate-supplemented medium (20 μM); □, HB101/pBR322 grown in the absence of molybdate and in the presence of 10 mM tungstate; ○, HB101/pBR322 grown in the absence of molybdate and in the presence of 100 mM tungstate; ▲, HB101/pDMS160 grown in the absence of molybdate and in the presence of 10 mM tungstate; ■, HB101/pDMS160 grown in the absence of molybdate and in the presence of 100 mM tungstate.

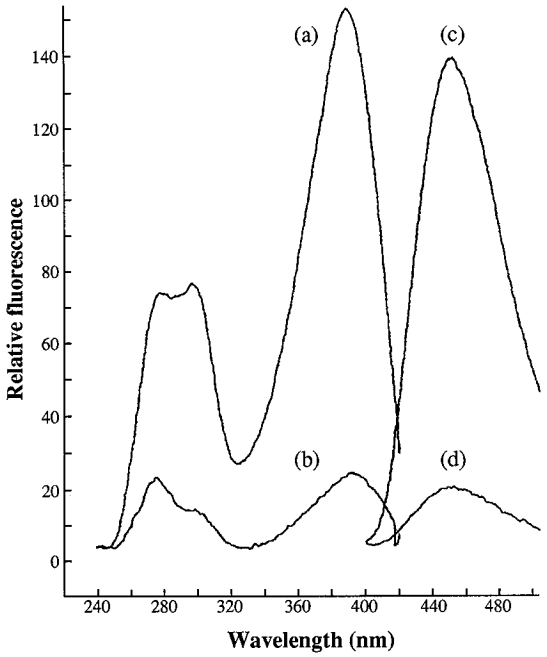

FIG. 3. Fluorescence spectra of form A MPT extracts from membranes containing DmsABC overexpressed in the presence of molybdate (a and c) and tungstate (b and d). Membrane protein (20 mg) was acid denatured and iodine oxidized. Excitation spectra (a and b) were recorded between 240 and 420 nm with an emission wavelength of 455 nm. Emission spectra (c and d) were recorded between 400 and 520 nm with an excitation wavelength of 380 nm. Spectra of membranes from HB101/pBR322 grown on GF minimal medium in the presence of 15 mM tungstate were used as baselines.

HB101/pBR322 cells grow at an equivalent rate in the absence of added molybdate (data not shown) (4), indicating that they are able to scavenge sufficient molybdate from the minimal medium to support respiratory growth on DMSO. In the presence of 10 and 100 mM tungstate, very little growth is detected, consistent with tungsten acting as a molybdenum antagonist. This contrasts with our previous study (4), in which 10 mM tungstate increased the length of the lag phase and significantly decreased the growth rate. This discrepancy is most likely due to the higher levels of molybdate in the minimal medium used in the earlier study. We have found that as little as 20 μM molybdate is sufficient to reverse the inhibitory effect of 10 mM tungstate (data not shown). A strain bearing the *dms* operon on a multicopy plasmid, HB101/pDMS160, is still able to grow slowly in the presence of 10 and 100 mM tungstate (Fig. 2), indicating that overexpression of DmsABC is able to partially overcome the inhibition of growth caused by high concentrations of tungstate.

Effect of tungstate on enzyme activity. Membranes containing overexpressed DmsABC from cells (HB101/pDMS160) grown in the presence and absence of tungstate (15 mM) have specific $BV\cdot^+$:TMAO oxidoreductase activities of 80.6 and 8.1 (μmol of $BV\cdot^+$ oxidized) (mg of membrane protein)$^{-1}$ min^{-1}. The effect of tungstate therefore appears to be to reduce the specific activity of DmsABC in membranes to approximately 10% of that found in cells grown in the presence of molybdate. The activity in membranes from cells with normal (chromosomal) expression of DmsABC (HB101/pBR322) grown in the presence of tungstate is 2.4 (μmol of $BV\cdot^+$ oxidized) (mg of membrane protein)$^{-1}$ min^{-1}. EPR spectra of the iron-sulfur clusters present in membranes containing overexpressed DmsABC from cells grown in the presence of molybdate and tungstate indicate that tungstate has little or no effect on the concentration of DmsABC accumulated in the cytoplasmic membrane (see below).

Effect of tungstate on Mo-MGD assembly into DmsABC. Molybdenum cofactor was released from *E. coli* membranes containing overexpressed DmsABC by acid hydrolysis followed by I_2 and KI oxidation and fluorescence assay of the form A MPT derivative (15). Figure 3 shows the effect of tungstate on the fluorescence spectra of acid-treated and iodine-oxidized membrane samples from HB101/pDMS160. Noticeable in the spectra of the form A extract of the molybdate-grown membranes are an excitation maximum at 390 nm and an emission maximum at 450 nm. These features are consistent with the presence of the form A MPT derivative in extracts from molybdate-grown membranes containing overexpressed DmsABC (15). The spectra of tungstate-grown membranes containing overexpressed DmsABC contain features similar to those found in the molybdate-grown membranes, but their intensities are approximately 14 to 16% of those of the molybdate-grown membranes.

EPR spectroscopy of membranes containing overexpressed DmsABC from cells grown in the presence of molybdate and tungstate. Figure 4 shows EPR spectra, recorded at 12 K, of membranes containing overexpressed DmsABC from cells grown in the presence of tungstate. The EPR spectrum of dithionite-reduced membranes (Fig. 4a) is essentially identical to that of membranes from HB101/pDMS160 cells grown in the presence of molybdate (not shown) and the previously reported spectrum of membrane-bound DmsABC (9, 25). This spectrum arises from the four [4Fe-4S] clusters ligated by four ferredoxin-like Cys groups in the sequence of DmsB. Double integrations of EPR spectra recorded under nonsaturating conditions show that the presence of tungstate has a negligible effect on the assembly of overexpressed DmsABC into the cytoplasmic membrane.

When the membranes of tungstate-grown cells are reduced with dithionite and then oxidized with 25 mM DMSO (Fig. 4b),

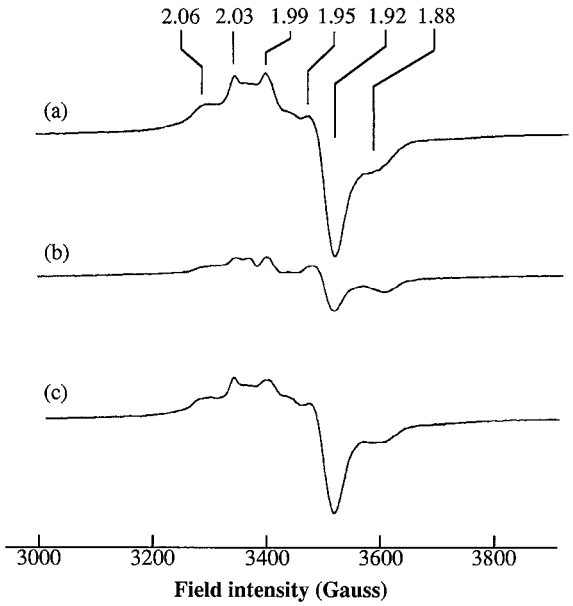

FIG. 4. EPR spectra of membranes containing overexpressed DmsABC from tungstate-grown cells. (a) Reduced with 5 mM dithionite. (b) Reduced with 5 mM dithionite and then oxidized with 25 mM DMSO. (c) Reduced with 25 mM dithionite and then oxidized in the presence of 0.2 mM HOQNO. Instrument conditions: temperature, 12 K; microwave power, 2 mW; microwave frequency, 9.45 GHz; modulation amplitude, 10 G_{pp} at 100 KHz; protein concentration, 30 mg ml^{-1}. Spectra are corrected for gain, tube calibrations, and protein concentrations.

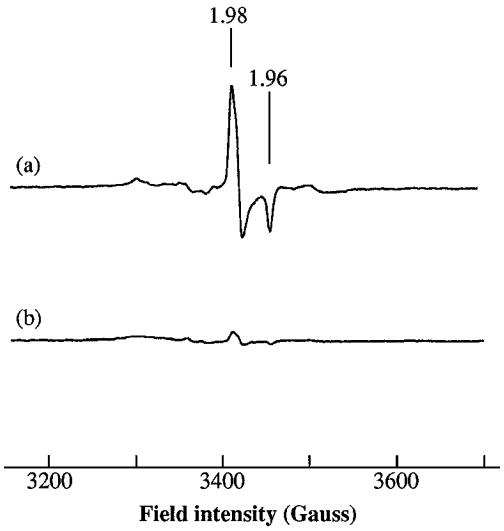

FIG. 5. EPR spectra of redox-poised membranes containing overexpressed DmsABC grown in the presence of molybdate (a) and tungstate (b). Instrument conditions: temperature, 100 K; microwave power, 20 mW; microwave frequency, 9.45 GHz; modulation amplitude, 2 G_{pp} at 100 KHz; protein concentration, 30 mg ml^{-1}; E_h, −64 mV (a) and −71 mV (b).

the intensity of the EPR spectrum is reduced significantly compared with the spectrum of the dithionite-reduced membranes (Fig. 4a). This suggests that some oxidation of the DmsABC [Fe-S] clusters is taking place in the presence of DMSO. This result bears comparison with the enzyme activity data and fluorescence data (Fig. 3), which suggest that the total population of DmsABC from tungstate-grown cells has approximately 10% of the activity and 15% of the MGD concentration of the population of DmsABC from molybdate-grown cells. There are two possibilities to explain these results. (i) All of the DmsABC from tungstate-grown cells has 10% of the activity of DmsABC from molybdate-grown cells. (ii) Ten percent of the DmsABC from tungstate-grown cells contains Mo-MGD and is fully active. Because the [4Fe-4S] clusters of Mo-MGD containing DmsABC are in equilibrium with both menaquinol and DMSO (25, 33), this would result in DMSO-dependent oxidation of all of the inactive DmsABC [4Fe-4S] clusters via the menaquinol pool. In order to test this possibility, we studied the effect of DMSO oxidation on the oxidation of the DmsABC [4Fe-4S] clusters in membranes from tungstate-grown cells in the presence of 0.2 mM 2-*n*-heptyl-4-hydroxyquinoline-*N*-oxide (HOQNO), an inhibitor of menaquinol oxidation by DmsABC (26). Figure 4c shows the EPR spectrum of membranes (plus 0.2 mM HOQNO) containing DmsABC from tungstate-grown cells reduced with dithionite and then treated with 25 mM DMSO. In this spectrum, there is only a minor diminution in the intensity of the [Fe-S] EPR spectrum, indicating that approximately 10% of the DmsABC from tungstate-grown cells is active and contains Mo-MGD.

Figure 5 shows redox-poised EPR spectra of membranes containing DmsABC from molybdate- and tungstate-grown cells recorded at 100 K. At a redox potential of around −60 mV, the spectrum of the Mo(V) reaches maximum intensity at pH 7 (9). Figure 5a shows the spectrum of membranes from molybdate-grown cells which has major features at g = 1.98 and g = 1.96. This spectrum is identical to that previously reported for the Mo(V) of DmsABC (9, 35). Figure 5b shows the equivalent spectrum of membranes from tungstate-grown cells. In this spectrum, the spectral features attributed to Mo(V) have an intensity that is approximately 8% of those found in the spectrum of molybdate-grown membranes. No evidence for additional W(V) signals was obtained throughout the redox range studied (−450 to +200 mV) in spectra recorded at both 12 and 100 K.

Characterization of DmsABC overexpressed in a *mob* mutant. Figure 6 shows fluorescence spectra of form A MPT extracts from membranes containing overexpressed DmsABC from a mob^+ strain (HB101/pDMS159 [Fig. 6a and c]) and a *mob* mutant strain (RK5208/pDMS159 [Fig. 6b and d]). The intensity of the emission and excitation maxima in spectra of form A MPT extracts of membranes from the *mob* mutant are much reduced compared with their intensities in the spectra of wild-type membranes. The emission maximum of the *mob* mutant spectrum is shifted to approximately 435 nm from approximately 450 nm in the wild-type spectrum. These spectra suggest that there is no Mo-MGD or Mo-MPT bound to DmsABC overexpressed in a *mob* mutant.

In order to corroborate the fluorescence data obtained with the *mob* mutant, EPR spectra of potentiometrically poised membrane samples containing overexpressed DmsABC were recorded (data not shown). Between −450 and +200 mV, no spectral features attributable to Mo(V) could be detected, indicating that the molybdenum is absent from and the four [4Fe-4S] clusters are present in DmsABC overexpressed in a *mob* mutant.

DISCUSSION

We have shown that the organic component of the molybdenum cofactor of *E. coli* DmsABC is MGD. This is in agreement with earlier results (4) and results presented herein that show that the *mob* gene product is required for assembly of active enzyme into the cytoplasmic membrane. The identifica-

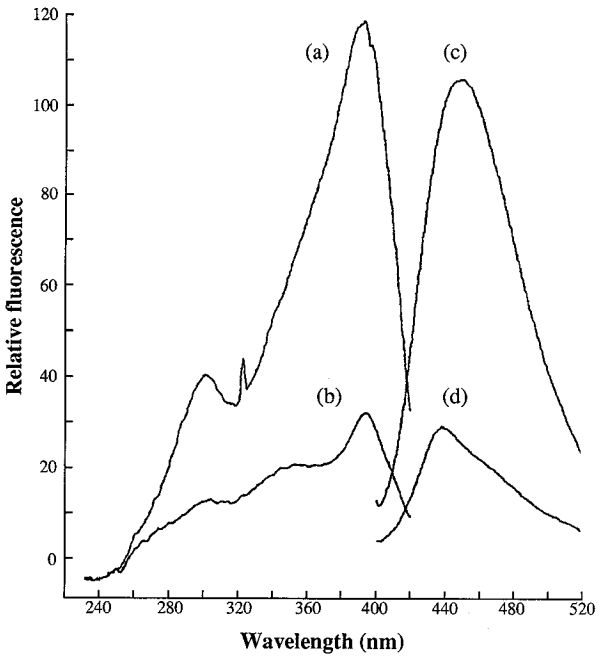

FIG. 6. Fluorescence spectra of extracts from membranes containing DmsABC overexpressed in a wild-type strain (a and c) and a *mob* strain (b and d). Samples were prepared and spectra were recorded as described for Fig. 3, except that no baseline spectrum was subtracted. Membranes were prepared from HB101/pDMS159 (a) and RK5208/pDMS159 (b).

tion of *mob*-dependent assembly of Mo-MGD into DmsABC supports a general model for molybdoenzyme assembly and activation in which *mob* is responsible for Mo-MGD assembly into a range of *E. coli* molybdoenzymes (15). The cofactor of DmsABC is identical to that found in the soluble, periplasmic DMSO reductase of *R. sphaeroides* (14). We have also shown that there is very little assembly of Mo-MGD into DmsABC in *E. coli* cells grown in the presence of tungstate and that the assembly of the organic components and assembly of the inorganic components of Mo-MGD into the enzyme appear to take place simultaneously.

Purified DmsABC contains approximately 0.26 mol of MGD per mol of enzyme. This compares with earlier mass spectroscopy measurements of the concentration of molybdenum present in purified preparations (0.34 mol of molybdenum per mol of DmsABC) (34). The presence of roughly equivalent concentrations of the organic and inorganic components of Mo-MGD in purified preparations also supports a model for MGD and metal insertion in which these events occur simultaneously (Mo-MGD being inserted as a single entity). The less-than-stoichiometric concentration of Mo-MGD led us to determine if the level of occupancy of Mo-MGD in DmsABC in membranes is higher than that in purified preparations. We measured the concentration of molybdenum in membranes from HB101/pDMS160 cells by mass spectroscopy and found that Mo is present stoichiometrically with the concentration of DmsABC estimated by EPR spin quantitations of the DmsB [Fe-S] signals (25a). Because DmsABC is the only major molybdenum-containing enzyme in membranes containing overexpressed DmsABC, it appears that a major proportion of Mo-MGD is either dissociated from the enzyme or is oxidatively destroyed during the enzyme purification procedure.

Inclusion of tungstate in GD minimal medium has been previously reported to inhibit anaerobic respiratory growth of *E. coli* (4). Our results (Fig. 2) corroborate this earlier work but add an interesting new dimension—that overexpression of the *dmsABC* operon appears to partially overcome inhibition by tungstate. Growth of *E. coli* HB101/pBR322 on GD minimal medium is strongly inhibited by 10 mM tungstate, but HB101/pDMS160 is able to grow at a tungstate concentration of 100 mM. This relief from inhibition by tungstate is probably the result of scavenging of the relatively small amounts of molybdate present in the media by the Mo-MGD biosynthetic pathway. The fluorescence, enzyme activity, and EPR data are consistent with the presence of tungstate (in the GF minimal medium) limiting the Mo-MGD occupancy of DmsABC to approximately 10% of that obtained when the cells are grown in the presence of molybdate. Because *E. coli* HB101/pDMS160 overexpresses DmsABC approximately 10-fold compared with HB101/pBR322 (5, 25), the overexpressing strain should have a concentration of active DmsABC approximately equivalent to the concentration present in HB101/pBR322 grown in the presence of molybdate. This concentration of active enzyme appears to be sufficient to support a slow rate of anaerobic growth of HB101/pDMS160 on glycerol-DMSO-tungstate medium. However, it is not clear why HB101/pDMS160 in the presence of 100 mM tungstate does not grow as well as HB101/pBR322 in the presence of molybdate. It would be interesting from the perspective of bacterial metal resistance to determine if similar overexpression-resistance phenomena are observed in other molybdoenzymes, such as *E. coli* NarGHI.

In the presence of tungstate, neither the organic component of Mo-MGD nor the metal is detected in DmsABC. The most likely explanation for this result is that MPT or MGD cannot be inserted into DmsABC. However, we cannot eliminate the possibility that metal-free or tungsten-containing cofactor is inserted into the apoenzyme in an unstable form which rapidly dissociates from the complex. However, the simplest explanation of the data is that the insertions of the organic and metal components of Mo-MGD appear to be very closely linked and probably occur at the same time. This result bears interesting comparison with those from studies of molybdoenzymes from bacteria which are able to ligate either molybdenum or tungsten (11, 29, 30) and studies of the hyperthermophilic archaeabacteria, in which the molybdenum cofactor-containing enzymes ligate tungsten in preference to molybdenum (16).

Mutations in the *mob* locus appear to prevent both nucleotide addition to Mo-MPT and Mo-MPT insertion into DmsABC. The *mob* locus has been shown to be responsible for guanine nucleotide attachment to Mo-MPT in *E. coli* molybdoenzymes (15). Santini et al. (27) proposed that in the case of NarGHI, Mo-MPT insertion precedes nucleotide addition. Our results with DmsABC indicate that the *mob* gene product is responsible for nucleotide addition prior to cofactor insertion. It is not clear why NarGHI with Mo-MPT bound is inactive in a *mob* mutant. It would be interesting to systematically study the effect of the *mob* locus on all of the *E. coli* molybdoenzymes to determine if they fall into two classes with respect to the effect of *mob* mutants: those which bind Mo-MPT prior to nucleotide addition (NarGHI) and those which bind Mo-MGD but not Mo-MPT (DmsABC).

Figure 7 shows a model for the assembly of the molybdenum cofactor into DmsABC. In Fig. 7, MPT is converted to Mo-MPT by the addition of molybdenum. It has been suggested that molybdenum is transported into *E. coli* as molybdate by the gene products of the *modABCD* operon (13). The *mog* locus has been implicated in the binding of molybdate to MPT (12, 17). The data presented herein show that the presence of tungsten prevents both molybdenum ligation to MPT and insertion of the organic component of the cofactor into

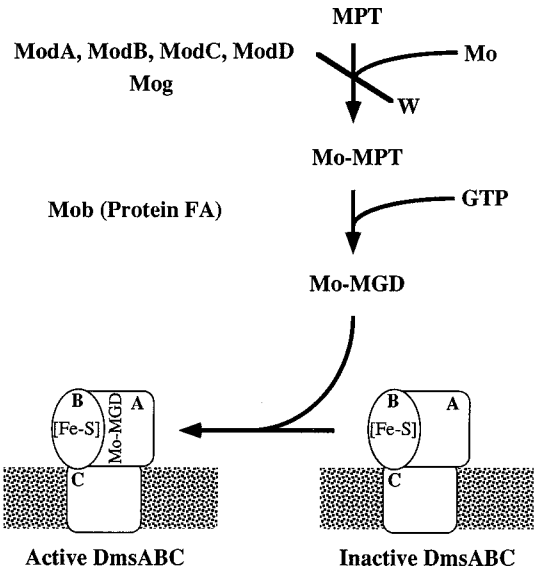

FIG. 7. Model for the final stages of Mo-MGD biosynthesis and insertion into DmsABC incorporating the results of this study. The accumulation and assembly of molybdate appear to be dependent on the *mod* operon (13, 24) and the poorly characterized *mog* locus (12, 17). Nucleotide attachment is dependent on the *mob* gene product (15, 21). Final activation of DmsABC may also involve a gene product equivalent to NarJ (8).

DmsABC. Previous studies of the effect of tungstate on *E. coli* NarGHI activation suggest that it causes the molybdenum cofactor to accumulate in either a tungsten-ligating form or as an empty cofactor (MPT) (1). We have shown that neither of these two potential forms of the cofactor is assembled into DmsABC. Our results with a *mob* mutant also indicate that in the case of DmsABC, nucleotide attachment must precede cofactor insertion, in contrast with what has been suggested for NarGHI (27). However, in the case of NarGHI, the enzyme studied was the soluble cytoplasmic NarGH dimer rather than the membrane-bound holoenzyme. It is possible in the case of the soluble DmsAB dimer (9) that cofactor insertion may also be possible prior to nucleotide addition. The DmsAB dimer is extremely labile, and we have been unable to generate a preparation stable enough to test this hypothesis (31a).

Overall, the data presented herein show that the molybdenum cofactor is present in *E. coli* DmsABC as Mo-MGD. Inclusion of tungstate in anaerobic growth media results in the assembly of DmsABC in which there appears to be a normal [4Fe-4S] cluster composition but no MGD, MPT, molybdenum, or tungsten. A mutation in the *mob* locus prevents cofactor assembly into DmsABC, suggesting that guanine nucleotide addition precedes cofactor insertion in the assembly pathway. The results have implications for the assembly and activation pathways of a large group of complex [Fe-S] molybdoenzymes which share the same overall molecular architecture as *E. coli* DmsABC (35).

ACKNOWLEDGMENTS

This work was funded by a grant from the Medical Research Council of Canada to J.H.W. (PG11440) and a National Institutes of Health grant to K.V.R. (GM00091). J.L.S. was supported by Graduate Studentships from the Natural Sciences and Engineering Research Council of Canada and the Alberta Heritage Foundation for Medical Research.

REFERENCES

1. **Amy, N. K., and K. V. Rajagopalan.** 1979. Characterization of molybdenum cofactor from *Escherichia coli*. J. Bacteriol. **140:**114–124.
2. **Berg, B. L., J. Li, J. Heider, and V. Stewart.** 1991. Nitrate-inducible formate dehydrogenase in *Escherichia coli* K-12. I. Nucleotide sequence of the *fdnGHI* operon and evidence that opal (UGA) encodes selenocysteine. J. Biol. Chem. **266:**22380–22385.
3. **Bilous, P. T., S. T. Cole, W. F. Anderson, and J. H. Weiner.** 1988. Nucleotide sequence of the *dmsABC* operon encoding the anaerobic dimethylsulphoxide reductase of *Escherichia coli*. Mol. Microbiol. **2:**785–795.
4. **Bilous, P. T., and J. H. Weiner.** 1985. Dimethyl sulfoxide reductase activity by anaerobically grown *Escherichia coli* HB101. J. Bacteriol. **162:**1151–1155.
5. **Bilous, P. T., and J. H. Weiner.** 1988. Molecular cloning and expression of the *Escherichia coli* dimethyl sulfoxide reductase operon. J. Bacteriol. **170:** 1511–1518.
6. **Blasco, F., C. Iobbi, G. Giordano, M. Chippaux, and V. Bonnefoy.** 1989. Nitrate reductase of *Escherichia coli*: completion of the nucleotide sequence of the *nar* operon and reassessment of the role of the alpha and beta subunits in iron binding and electron transfer. Mol. Gen. Genet. **218:**249–256.
7. **Blasco, F., C. Iobbi, J. Ratouchniak, V. Bonnefoy, and M. Chippaux.** 1990. Nitrate reductases of *Escherichia coli*: sequence of the second nitrate reductase and comparison with that encoded by the *narGHJI* operon. Mol. Gen. Genet. **222:**104–111.
8. **Blasco, F., J. Pommier, V. Augier, M. Chippaux, and G. Giordano.** 1992. Involvement of the *narJ* or *narW* gene product in the formation of active nitrate reductase in *Escherichia coli*. Mol. Microbiol. **6:**221–230.
9. **Cammack, R., and J. H. Weiner.** 1990. Electron paramagnetic resonance spectroscopic characterization of dimethyl sulfoxide reductase of *Escherichia coli*. Biochemistry **29:**8410–8416.
10. **Condon, C., and J. H. Weiner.** 1988. Fumarate reductase of *Escherichia coli*: an investigation of function and assembly using *in vivo* complementation. Mol. Microbiol. **2:**43–52.
11. **Deaton, J. C., E. I. Solomon, G. D. Watt, P. J. Wetherbee, and C. N. Durfor.** 1987. Electron paramagnetic resonance studies of the tungsten-containing formate dehydrogenase from *Clostridium thermoaceticum*. Biochem. Biophys. Res. Commun. **149:**424–430.
12. **Hinton, S. M., and D. Dean.** 1990. Biogenesis of molybdenum cofactors. Crit. Rev. Microbiol. **17:**169–188.
13. **Johann, S., and S. M. Hinton.** 1987. Cloning and nucleotide sequence of the *chlD* locus. J. Bacteriol. **169:**1911–1916.
14. **Johnson, J. L., N. R. Bastian, and K. V. Rajagopalan.** 1990. Molybdopterin guanine dinucleotide: a modified form of molybdopterin identified in the molybdenum cofactor of dimethyl sulfoxide reductase from *Rhodobacter sphaeroides* forma specialis denitrificans. Proc. Natl. Acad. Sci. USA **87:** 3190–3194.
15. **Johnson, J. L., L. W. Indermaur, and K. V. Rajagopalan.** 1991. Molybdenum cofactor biosynthesis in *Escherichia coli*. Requirement of the *chlB* gene product for the formation of molybdopterin guanine dinucleotide. J. Biol. Chem. **266:**12140–12145.
16. **Johnson, J. L., K. V. Rajagopalan, S. Mukund, and M. W. Adams.** 1993. Identification of molybdopterin as the organic component of the tungsten cofactor in four enzymes from hyperthermophilic Archaea. J. Biol. Chem. **268:**4848–4852.
17. **Kamdar, K. P., M. E. Shelton, and V. Finnerty.** 1994. The *Drosophila* molybdenum cofactor gene *cinnamon* is homologous to three *Escherichia coli* cofactor proteins and to the rat protein gephyrin. Genetics **137:**791–801.
18. **Krafft, T., M. Bokranz, O. Klimmek, I. Schröder, F. Fahrenholz, E. Kojro, and A. Kröger.** 1992. Cloning and nucleotide sequence of the *psrA* gene of *Wolinella succinogenes* polysulphide reductase. Eur. J. Biochem. **206:**503–510.
19. **Lowry, O. H., N. J. Rosebrough, A. L. Farr, and R. J. Randall.** 1951. Protein determination with the Folin phenol reagent. J. Biol. Chem. **191:**265–275.
20. **Markwell, M. A., S. M. Haas, L. L. Bieber, and N. E. Tolbert.** 1978. A modification of the Lowry procedure to simplify protein determination in membrane and lipoprotein samples. Anal. Biochem. **87:**206–210.
21. **Plunkett, G., V. Burland, D. L. Daniels, and F. R. Blattner.** 1993. Analysis of the *Escherichia coli* genome. III. DNA sequence of the region from 87.2 to 89.2 minutes. Nucleic Acids Res. **21:**3391–3398.
22. **Rajagopalan, K. V., and J. L. Johnson.** 1992. The pterin molybdenum cofactors. J. Biol. Chem. **267:**10199–10202.
23. **Rajagopalan, K. V., J. L. Johnson, M. M. Wuebbens, D. M. Pitterle, J. C. Hilton, T. R. Zurick, and R. M. Garrett.** 1993. Chemistry and biology of the molybdenum cofactors. Adv. Exp. Med. Biol. **338:**355–362.
24. **Rech, S., U. Deppenmeyer, and R. P. Gunsalus.** 1994. Regulation of the *modABCD* (*chlD*) operon of *Escherichia coli* by molybdate, abstr. H4, p. 200. *In* Abstracts of the 94th General Meeting of the American Society for Microbiology 1994. American Society for Microbiology, Washington, D.C.
25. **Rothery, R. A., and J. H. Weiner.** 1991. Alteration of the iron-sulfur cluster composition of *Escherichia coli* dimethyl sulfoxide reductase by site-directed mutagenesis. Biochemistry **30:**8296–8305.

25a. **Rothery, R. A., and J. H. Weiner.** Unpublished results.

26. **Sambasivarao, D., and J. H. Weiner.** 1991. Dimethyl sulfoxide reductase of

Escherichia coli: an investigation of function and assembly by use of in vivo complementation. J. Bacteriol. **173:**5935–5943.

27. **Santini, C.-L., C. Iobbi-Nivol, C. Romane, D. H. Boxer, and G. Giordano.** 1992. Molybdoenzyme biosynthesis in *Escherichia coli*: in vitro activation of purified nitrate reductase from a *chlB* mutant. J. Bacteriol. **174:**7934–7940.
28. **Saracino, L., M. Violet, D. H. Boxer, and G. Giordano.** 1986. Activation in vitro of respiratory nitrate reductase of *Escherichia coli* K12 grown in the presence of tungstate. Involvement of molybdenum cofactor. Eur. J. Biochem. **158:**483–490.
29. **Schmitz, R. A., S. P. Albracht, and R. K. Thauer.** 1992. Properties of the tungsten-substituted molybdenum formylmethanofuran dehydrogenase from *Methanobacterium wolfei*. FEBS Lett. **309:**78–81.
30. **Schmitz, R. A., S. P. Albracht, and R. K. Thauer.** 1992. A molybdenum and a tungsten isoenzyme of formylmethanofuran dehydrogenase in the thermophilic archaeon *Methanobacterium wolfei*. Eur. J. Biochem. **209:**1013–1018.
31. **Shanmugam, K. T., V. Stewart, R. P. Gunsalus, D. H. Boxer, J. A. Cole, M. Chippaux, J. A. DeMoss, G. Giordano, E. C. Lin, and K. V. Rajagopalan.** 1992. Proposed nomenclature for the genes involved in molybdenum metabolism in *Escherichia coli* and *Salmonella typhimurium*. Mol. Microbiol. **6:**3452–3454.

31a. **Simala Grant, J. L., and J. H. Weiner.** Unpublished results.

32. **Stewart, V., and C. H. MacGregor.** 1982. Nitrate reductase in *Escherichia coli* K-12: involvement of *chlC*, *chlE*, and *chlG* loci. J. Bacteriol. **151:**788–799.
33. **Trieber, C. A., R. A. Rothery, and J. H. Weiner.** 1994. Multiple pathways of electron transfer in dimethyl sulfoxide reductase of *Escherichia coli*. J. Biol. Chem. **269:**7103–7109.
34. **Weiner, J. H., D. P. MacIsaac, R. E. Bishop, and P. T. Bilous.** 1988. Purification and properties of *Escherichia coli* dimethyl sulfoxide reductase, an iron-sulfur molybdoenzyme with broad substrate specificity. J. Bacteriol. **170:**1505–1510.
35. **Weiner, J. H., R. A. Rothery, D. Sambasivarao, and C. A. Trieber.** 1992. Molecular analysis of dimethylsulfoxide reductase: a complex iron-sulfur molybdoenzyme of *Escherichia coli*. Biochim. Biophys. Acta **1102:**1–18.